RADOME BORESIGHT ERROR AND COMPENSATION TECHNIQUES FOR ELECTRONICALLY SCANNED ARRAYS

Donald Peterson, James Otto, and Kenea Douglas
R. F. Systems Branch
Naval Air Warfare Center Weapons Division, China Lake, CA 93555-6001

Abstract

This paper describes work performed to evaluate precision beam control using an electronically scanned array antenna. The primary factors that limit beam pointing accuracy, both with and without a radome, are discussed. Laboratory measurements show the effects of a radome. Boresight errors and beamshape distortion were measured. Processes were evaluated that showed the capability to correct angle error as well as to restore beamshape.

Introduction

This work was carried out under the Millimeter Wave Seeker Program in coordination with the Army Strategic Defense Command (SDC), sponsored by the Strategic Defense Initiative Office (SDIO). The technical requirements were focused on SDIO's ENDO LEAP technology demonstration program.

Radome induced boresight error (BSE) and BSE slope (BSES) are usually the dominant errors that limit angle accuracy of a radar system. For a missile system with proportional navigation, BSES is the more important error. The boresight error slope interacts with the missile guidance loop. A negative slope leads to an under damped tracking loop, creating instabilities during maneuvers. A positive slope leads to an over damped system and an underresponsive tracking loop.

Objectives of the present study were guided by requirements[1] of an interceptor against a tactical ballistic missile, in particular an ENDO LEAP type interceptor vehicle. ENDO LEAP requires hit-to-kill and aimpoint selection. Hit-to-kill requires extremely accurate angle tracking. The seeker antenna is expected to be an electronically scanned array (ESA) functioning at millimeter wave frequencies (35 GHz or 94 GHz).

BSE and BSES Requirements

For the ENDO LEAP application, boresight error slope (BSES) is the most important factor in achieving hit-to-kill. A rigorous determination of minimal required BSES requires a very good simulation, probably in a 6 degree-of-freedom (DOF) model involving many system parameters. This is beyond the scope of this study. However ENDO LEAP contractor analyses indicate that BSES of perhaps as low as 0.1% to 0.2% may be required. Initial analyses indicate that uncompensated BSES may be as high as 10%. Removal of 99% of BSES will be very difficult. Some industry measurements indicate that maximum BSES is inversely proportional to number of wavelengths across the aperture. Figure 1 represents data for several typical uncompensated, untailored missile radomes that operate at different frequencies and aperture sizes. Radome fineness ratio for the radomes represented by the figure varied between 2 and 3. W-band (94 GHz) is seen to have a distinct advantage compared to lower frequencies. For example, a 15 cm diameter aperture gives 47 wavelengths across the aperture. In this case, uncompensated BSES is less than 1%.
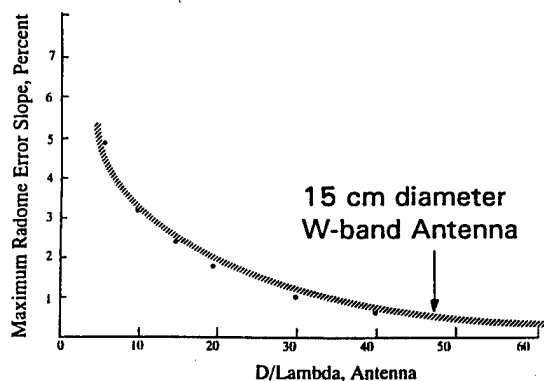

Figure 1. Uncompensated Boresight Error Slope as a Function of Antenna Aperture in Wavelengths. Reproduced by permission of R. Miller of Hughes Aircraft Co., Reference 2.

The BSE requirement is less well defined. The expected BSE requirement is a few hundred microradians or less. BSES is directly related to BSE such that any reduction in BSE can be expected to likewise reduce BSES. Note in

4619

further discussions that the term BSE in general is assumed to include the very important BSES that is derived directly from plotted BSE data.

High angle accuracy depends on three major system factors; (a) precision beam forming and control, (b) static BSE compensation, and (c) dynamic BSE compensation. The majority of this report covers the first two factors. Investigation of the latter, dynamic BSE compensation, was being investigated in a joint effort with industry when this program was terminated.

Precision Beamforming

Electronically Scanned Array (ESA) technology has been the subject of numerous recent studies[3,4]. An ESA has some basic advantages over the conventional gimbal mounted antenna because the wavefront can be corrected for both angle of arrival (pointing angle) and wavefront distortion (beamshape). Correction of wavefront distortion can sharpen the monopulse tracking null and reduce sidelobes. Low sidelobes or control of position of adaptive side-nulls is important because extraneous noise or signals entering the sidelobes can degrade angle accuracy[5]. Beam shape is readily controllable with an ESA because phase and magnitude are controllable to each radiating element, allowing control of beamwidth and sidelobes.

Degrading factors are also introduced by the nature of the ESA. Due to the digitally controlled phase, the phase front will not be linear, but will be a saw tooth shape. This introduces scattering out of the main beam, resulting in null filling, raised sidelobes, and possibly null angle shift.

Beam pointing is the more important factor for the present application. First, the basic beam steering relation for an ESA is:

$$\Phi i = (360/\lambda) [Xi \sin(Ac) - Yi \sin(Bc)] \qquad \text{Eq. (1)}$$

where;
Φi = phase shift in degrees for module i.
Xi, Yi = location of module i with respect to the array center, in mm
λ = wavelength in mm
Ac, Bc = commanded azimuth and elevation angles.

The primary factors that limit pointing accuracy (no radome) are discussed briefly below.
(1) Element phase error. Pointing error, σ(point), is directly proportional to the rms phase error, and inversely related to the square root of the

number of independent radiating elements in the ESA[6]:

$$\sigma(\text{point}) = \frac{\sigma(\text{phase})}{K\sqrt{Ne}} \qquad \text{Eq. (2)}$$

where:
σ(point) = rms boresight error
σ(phase) = rms phase error
K = monopulse difference slope
  $= (\pi/2)/\theta_{bw}$, for a circular aperture
  $= (\pi/\sqrt{3})/\theta_{bw}$, for a square aperture
θ_{bw} = beamwidth (at -3 dB)
Ne = Number of elements whose error output is uncorrelated

Note: The phase error is the root-sum-square (RSS) total of all phase error contributors, such as quantization error, error caused by inaccurate positioning of elements in three dimensions, etc. The rms phase quantization error due to the quantization interval $2\pi/(2^B)$ is:

$$\sigma(\text{phase/quant}) = \frac{2\pi}{2^B \sqrt{12}} \qquad \text{Eq. (3)}$$

where: B = number of bits.

(2) Quantized beam stepping. An ESA is a body-fixed system; the antenna is not gimbaled to stare at the target, rather the antenna is fixed in the forward direction. Further, with digitally controlled phase, there is a granularity in beam stepping. In addition, some tracking methods arbitrarily use larger beam stepping increments. The off-null tracking angle introduces angle error[7]:

$$\sigma(\text{point}) = \frac{\theta_{bw}}{K_m \sqrt{2\,S/N}} \sqrt{1 + \left(K_m \frac{\theta}{\theta_{bw}} \right)^2} \qquad \text{Eq. (4)}$$

where:
σ(point) = rms pointing angle error
θ = look angle with respect to boresight
K_m = normalized monopulse difference slope
  $\cong 2.2$ for a circular aperture
S/N = signal/noise ratio

For example, for a target 10 mr off boresight, K_m of 2.2, and beamwidth of 25 mr, angle error

2

Accession Number: 4619

Publication Date: Jun 06, 1993

Title: Radome Boresight Error and Compensation Techniques for Electronically Scanned Arrays

Personal Author: Peterson, D.; Otto, J.; Douglas, K.

Corporate Author Or Publisher: U.S. Naval Air Warfare Center, China Lake, CA Report Number: AIAA 93-2648

Comments on Document: 2nd Annual AIAA SDIO Interceptor Technology Conference, June 6-9, 1993 at Albuquerque, NM

Descriptors, Keywords: Radome Boresight Error Compensation Electronics Scan Array Antenna ENDOLEAP ESA Endoatmosphere LEAP Interceptor Sensor Guidance Acquisition Track

Pages: 00008

Cataloged Date: Aug 05, 1993

Document Type: HC

Number of Copies In Library: 000001

Record ID: 27999

Source of Document: AIAA

would be multiplied by a factor of 1.33. Hatcher[8] and J. Frank[9] have investigated the granularity in beam positions. Note that both the Hatcher and the Frank investigations are theoretical and assume perfect placement of the radiating elements and no radome phase error. With random phase error, element to element, as seen in practice, much of this effect will be buried in noise because switching of phase shifters will have a random error superimposed upon them, and will not shift phase states at the exact phase expected by theory. Further relations pertaining to beam pointing error are covered in the Radar Handbook[10].

(3) Beam squint with frequency. The beam will squint in angle when frequency changes according the following relation:

$$\delta\theta = \tan(\theta)\, df/f, \qquad \text{Eq. (5)}$$

where
θ = look angle with respect to boresight,
f = frequency,
df/f = fractional frequency bandwidth that the waveform is scanned through.

Static BSE Contributors

The two dominant contributors to static radome BSE are; (a) beam angle deflection by the radome, and (b) radome blockage (e.g. hardened tip). Beam angle deflection is the major contributor to BSE and is caused by variations in the radome thickness and material properties throughout the radome. This is the conventional BSE that is usually corrected by carefully measuring BSE in the laboratory. This often entails BSE measurements over 1000 or more angular points. From this a BSE correction look-up table is created.

Radome blockage has two potential effects on a monopulse tracking radar. First, the monopulse quadrants will be unevenly illuminated. For a phase monopulse, this does not cause BSE, rather only causes null filling because only magnitudes of the monopulse outputs are affected, not phase. This can reduce one monopulse vector magnitude with respect to the other, raising the null value when the vectors are 180 degrees out of phase for the boresight case.

Second, blockage can cause BSE by means of phase distortions caused by diffraction about the radome blockage. This shifts the phase of one monopulse vector with respect to the other. This

BSE will vary with look angle through the radome. White and Overfelt[11] have found significant BSE due to a hardened radome tip. Feeman and Van Blaricum[12] are further studying the problem under a contract with the Naval Air Warfare Center.

Static BSE Compensation

In the past, BSE has been corrected only for pointing angle. The BSE compensation method has been precision measurement of BSE in a laboratory, often requiring measurement at a thousand or more angular points. This type of compensation does nothing for null filling and other beam distortions caused by the radome. Electronic scanned arrays (ESAs) add a new compensation capability; control of both phase and amplitude for each radiation element in the array. Measurements have shown that control of phase and amplitude can dramatically improve beam shape that is distorted by a poor radome, in addition to providing BSE compensation. These results are presented in this work.

Dynamic BSE Contributors

The most important contributors to dynamic BSE are: (a) thermal gradients, (b) aerothermal effects, (c) polarization effects, (d) radome flexure, (e) radome ablation, (f) rain and ice erosion, and (g) vibration.

Thermal gradients are caused by high velocity travel through the atmosphere. Heat and heat distribution will depend on velocity, altitude, and angle of attack and therefore, in general the thermal gradients will be very asymmetrical.

Aerothermal effects are due to the flow field about the radome. The flow field is composed of both neutral and ionized components. The more important effect for millimeter waves is formation of a plasma that can begin to occur at velocities of approximately 3 km/sec. For the ENDO LEAP velocity of 2 km/sec, BSE effects due to plasma are expected to be small and perhaps negligible.

Polarization effects present a very difficult problem because they are dependent on target characteristics and target orientation. Therefore return polarization characteristics will not be well known in general. Since the radome's BSE varies with incident polarization, there are presently no means to compensate for polarization induced BSE. Hall and White[13] have studied this problem and offer possible methods for reducing the

undesired effect, by use of an external polarization grid on the radome.

Heating, ablation and erosion can cause large changes in BSE. These problems have been investigated in classified programs such as the Extended Range INtercept Technology (ERINT) program and in work at Johns Hopkins University.

The antenna assembly flexes and vibrates during high G maneuvers. Phase errors introduced by this will be difficult to correct, except perhaps with adaptive BSE compensation methods. The system should be structurally designed to avoid significant flexure and vibration.

Dynamic BSE Compensation

The two approaches to dynamic BSE compensation are; (a) predictive, and (b) adaptive. Predictive compensation requires very accurate modeling of BSE throughout the tracking phase of the missile. At this time attempts are being made by industry[14,15] to model thermal gradients, ablation, and erosion. In some cases, the very difficult modeling effort can be simplified. For example, thermal gradients will be difficult to model. One solution is to spin the missile on its axis at a few revolutions per second whereby the thermal gradients will become averaged out and symmetrical about the missile axis, making the modeling task much simpler. In the predictive compensation method, BSE would be modeled as a function of the major parameters such as; (a) velocity, (b) altitude, (c), angle of attack, and (e) look angle through the radome.

The most desirable method of BSE compensation is adaptive whereby BSE error is sensed and automatically corrected, real time through the flight. This is an extremely difficult problem that has been studied for tens of years, with little significant progress to date. A survey of the problem and some candidate techniques were included in work published by Johns Hopkins University in 1980[16]. Raytheon Company has investigated limitations on accuracy of BSE compensation in some classified work. Some progress appears to have been made recently, intimately involving the missile guidance loop, in work by Johns Hopkins University and by Teledyne Brown, in classified work.

The ERINT program is developing adaptive methods. The majority of the BSE is removed by the standard methods of look-up tables of ambient BSE. Next, in-flight BSE is removed by predictive methods. The residual BSE is compensated by an adaptive method that interacts with the guidance control loop. Observer states in the form of Kalman filters in the guidance loop are used to sense perturbations due to the BSE slope during the end game maneuver and the final guidance corrections are made.

Laboratory Measurement Facilities

Boresight error measurements were made and compensation process were tested with an electronic scanned array (ESA) in two ranges; (a) a compact RF range, and (b) a near field range. The ESA consisted of 40 transmit/receive (T/R) modules, used in receive only mode, at 9.5 GHz. The T/R modules have 5 bits of phase control and 8 bits of attenuation (amplitude) control. Radiating elements are flared notch radiators, spaced at one-half wavelength intervals. The original X-band array is described in more detail in two reports[17,18].

ESA Calibration Process

The goal of the calibration process is a lookup table containing the input phase and amplitude states required for each element to produce the complex I and Q output values that steer the beam in the desired direction, according to the basic beam steering relation (Eq. 1). Element output phase, Φ, is related to I and Q by $\tan(\Phi) = I/Q$.

Output phase is not a simple, linear function of commanded input phase. Phase error is introduced by nonlinear response of the T/R modules, interaction between phase and amplitude settings, variation in location of radiating elements, etc. Calibration is required to correct for these system errors. The calibration process is a general method that allows much of the radome BSE to be removed. The calibration process that has been developed in our laboratory is described in more detail in Appendix A.

Precision Beamforming and Control Measurements

The extreme pointing accuracy requirements of hit-to-kill bring out a new set of effects that are normally ignored in a radar system. The following effects were investigated.

a. Phase shifter quantization error. The quantized phase shifters introduce phase error into the phase front, which in turn leads to an rms pointing error. The calibration process limits maximum phase error to intervals of width $2\pi/2^B$ and rms phase error to: $\sigma = 2\pi/(2^B\sqrt{12})$, Eq. 3, where B = number of bits. For 5 bits, the quantization interval is 11.25° (± 5.12°) and $\sigma = 3.2°$. Phase error was measured and the plotted results are shown in Figure 2. The phase error conforms to theory. Note the two bad elements, numbers 1 and 34, that are dead.

Figure 2. Phase Error, Element to Element, Across the Aperture. No Radome. Note that Elements #1 and #34 are Inoperative

Four bits or more is sufficient to limit rms beam pointing error to levels that satisfy the angle accuracy requirement, at Ka and W-bands, with a large number of independent radiating elements. For a laboratory confirmation, measurements with 4 and 5 bits found beam pointing error effects were buried in noise and not measurable. Equation (2) provides an estimate of 1.9 mrad pointing error due to 4 bits phase quantization error, with a square aperture, 40 independent radiating elements, at X-band ($\lambda = 32$ mm), with a 584 mm wide aperture.

b. System errors. Small errors become significant (mutual coupling, noise, phase noise, system non-linearities, phase/attenuation interdependence, temperature and time dependence, element radiation patterns, etc).

c. Beam squint. Squint has been observed at broadside where theoretically it should not occur. Imperfect phase shifters are suspected. Recalibration at closer frequency intervals may be required.

d. Superposition. The system response appears to be non-linear. The total output does not equal the sum of outputs activated and measured one at a time. However, at this time it appears this is not due to a non-linear system, but rather due to unequal phase responses through each receiving channel. Each channel is composed of several elements including T/R module, attenuator, and combiner, each contributing to phase imbalance. Phase balancing is done to approximately the one bit level of 11.25 degrees, but a residual unbalance remains.

e. Separability. Separation of variables may not be achievable. Interactions occur between variables. For example phase shift depends on element amplitude setting and frequency.

The latter four effects were observed in the laboratory but quantitative data is not available because the program was terminated. The effects require futher study.

Radome Measurements and Compensation Measurements

For these measurements, the 40 T/R modules were arranged to drive an array of 40 by 16 radiating elements, consisting of 40 active elements across with 16 elements vertical. Each 16 element column of radiating elements was hardwired to one of the 40 T/R modules. Thus there is beam control only in the horizontal direction. With our limited number of T/R modules, this allows measurements with beam shape more typical of a millimeter wave hit-to-kill seeker.

The T/R modules limit the present compensation process. There is large variability in sensitivity of the modules such that an even weighting across the aperture is impossible. As an alternative the aperture was weighted symmetrically about the center of the aperture, as described in Appendix A. The weighted magnitude response function for the aperture is shown in Figure 3. Note the symmetry about the center of the aperture. The weighting procedure compares symmetrical pairs of elements and reduces the magnitude of the stronger element to the magnitude of the opposite sided element. Also note that modules #1 and #34 are dead and that therefore modules #7 and #40 are likewise attenuated to produce symmetry. This weighting process raises the beam sidelobes, but optimizes power gain for the condition of modules available to us.

An alternative weighting method was used earlier, in which an even weighting across the aperture was attempted. Ignoring the two dead elements, all element power output was limited to the weakest element output. This excessively

reduced output power and lowered signal/noise to the point where useful measurements often could not be made.
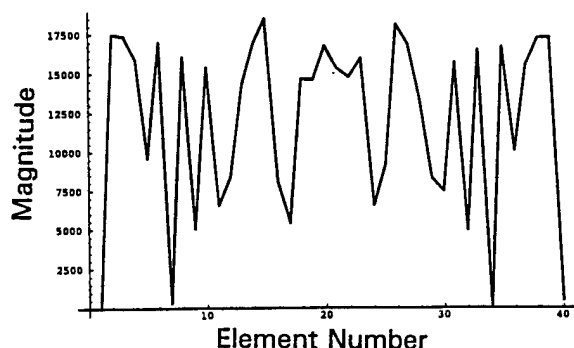

Figure 3. Aperture Weighting, for Symmetrical Weighting. Modules #1 and #34 are Inoperative. Therefore, Symmetrical Counterpart Elements #7 and #40 Were Given Maximum Attenuation.

Boresight error compensation

A crude radome was fabricated of Plexiglas, designed for scanning in only the horizontal direction with the 40X16 element linear array. Measurements were made in the compact range, of beam shape and BSE through this radome. The method used for beamshape restoration and BSE compensation was a recalibration process performed after the radome was added. This process was adapted from the calibration process described in Appendix A.

The sidelobes were strongly affected by the distorted radome, as shown in Figure 4 for the sum beam and Figure 5 for the monopulse difference pattern. In each figure, the beamshape is shown with no radome, with the Plexiglas radome, and the restored beamshape after compensation. The sidelobes were strongly affected by the distorted radome. In free space, the first sidelobes were down approximately 13 dB. With the Plexiglas radome in place, the beam was distorted and the sidelobes rose to -8 dB. The calibration-compensation process restored much of the beam shape and brought the sidelobes back down to approximately -12 dB. The ability to better restore the beamshape was limited by the high variability in sensitivity of the T/R modules, as described above.

The results of BSE measurements are shown in Figure 6, where boresight error is plotted with no radome, with the Plexiglas radome, and after compensation. Uncompensated boresight error through this radome was large, approximately
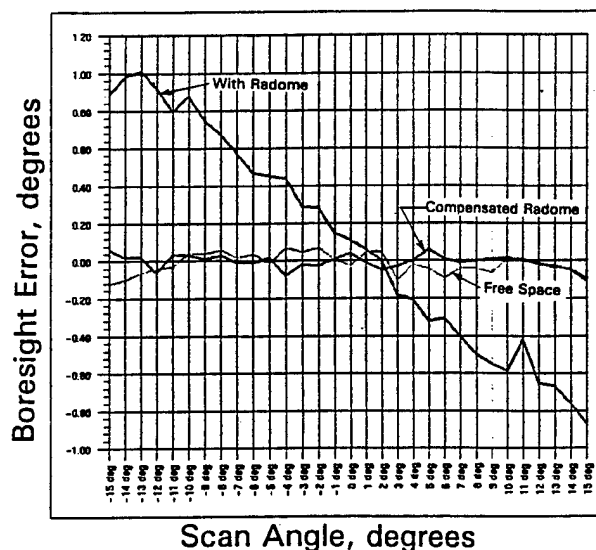

Figure 6. Boresight Error Compensation

1 degree at 15 degrees scan off of broadside. Boresight error slope is approximately 6.7%, average. The recalibration type of BSE compensation was able to reduce this error to approximately 0.04 degrees (0.7 mrad) rms, with approximately zero mean error, the same as for free space (no radome).
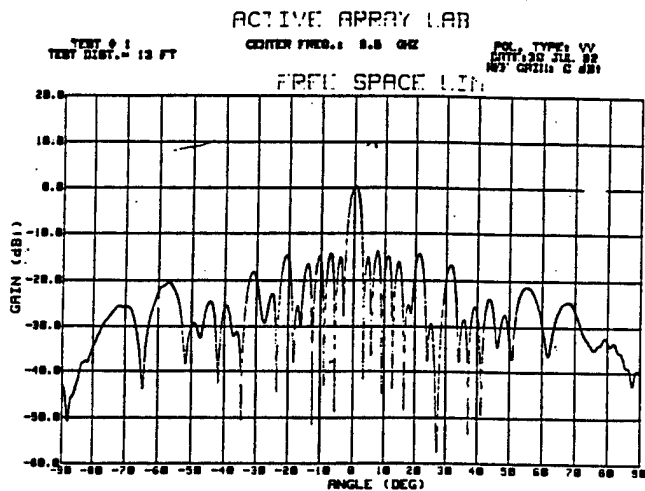
Conclusions

Processes have been evaluated in the laboratory that showed the capability to correct angle error as well as beamshape distortions that are caused by a radome, for an electronically scanned array. These compensations have been done under static laboratory conditions. Also, precision beam steering (no radome) was investigated and important sources of errors were found, such as beam squint with frequency at broadside, and effects of small system errors. These beam steering effects need to be further investigated. Further, the extremely important dynamic in-flight boresight errors must be investigated and means to compensate for these errors need to be developed.
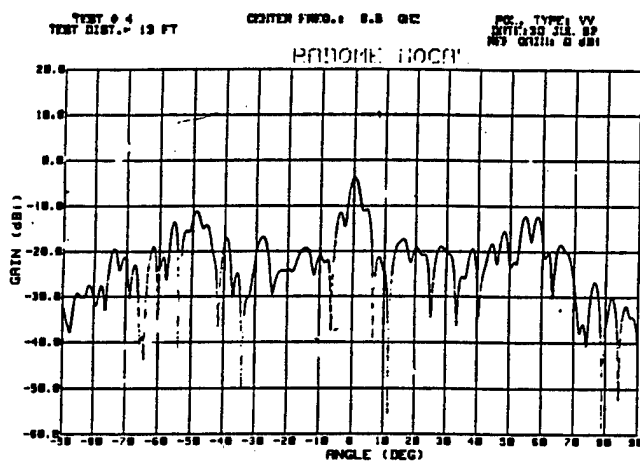
APPENDIX A: ESA Calibration Process
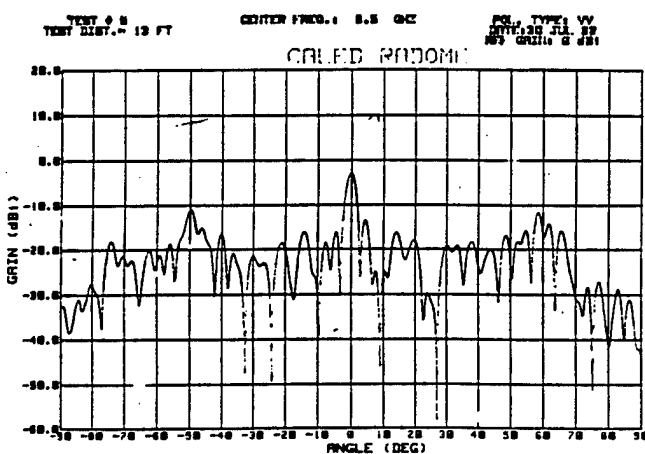
General

The goal of the calibration process is a lookup table containing the input phase and amplitude
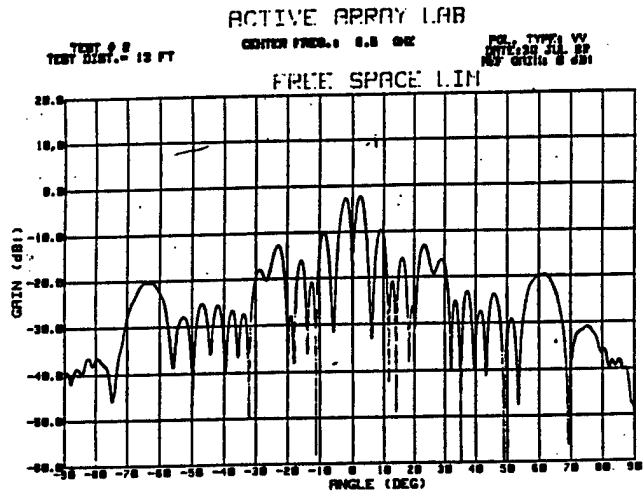
6

a. Beamshape in free space
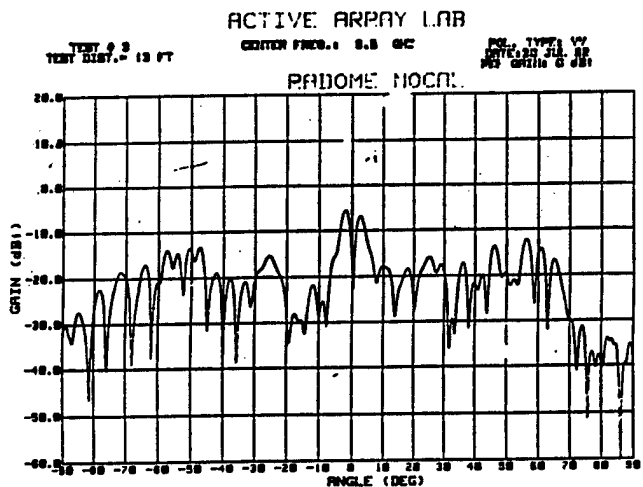

b. Beamshape with Plexiglas radome.
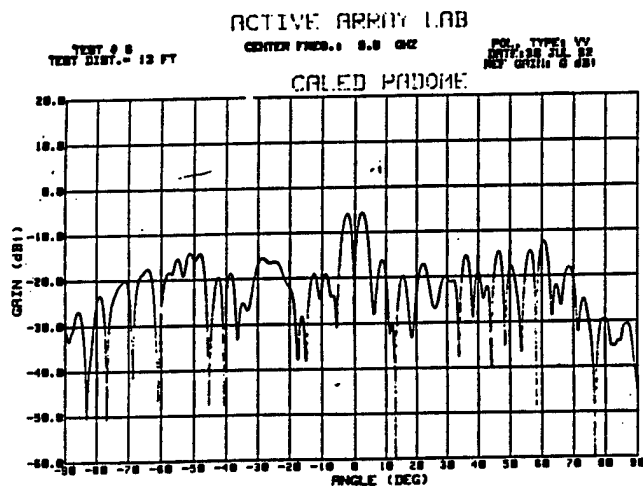

c. Restored Beamshape

Figure 4. Beamshape Restoration, Monopulse Sum Pattern

a. Beamshape in free space

b. Beamshape with Plexiglas radome

c. Restored Beamshape

Figure 5. Beamshape Restoration, Monopulse Difference Pattern

7

states required for each element to produce the complex I and Q output values that steer the beam in the desired direction, according to the basic beam steering relation (Eq. 1). Element output phase, Φ, is related to I and Q by $\tan(\Phi) = I/Q$.

Output phase is not a simple, linear function of commanded input phase. Phase error is introduced by nonlinear response of the T/R modules, interaction between phase and amplitude settings, variation in location of radiating elements, etc. Calibration is required to correct for these system errors. The calibration process that has been developed in our laboratory is described below.

The general process is to first collect the element response data in two files that will be used in the calibration; a system data file and an element data file. Except for mechanical alignment, these processes have been automated. Since the system drifts, data for the system file is recollected frequently, once or more per day if required. However the T/R module response curve as a whole has been found to be relatively stable, although the response curve as a whole may shift. Therefore complete element data need only be collected every few days.

A. Data Collection

Depending on whether a full element calibration or a faster system calibration will be done, data is collected into either; (I) Combined System/Element data file, or (II) System data file. In either case, the ESA is first set up for measurements as follows.
(a) Produce plane waves incident onto the ESA at a power level below the saturation power (1 dB compression point) of the ESA. In our lab, plane waves are produced via our compact antenna range.
(b) Align the ESA at a known angle with respect to the plane wave, usually with the ESA boresight aligned normal to the plane wave (i.e. broadside to the plane wave). Data is collected as complex I and Q data, measured at the output of the RF manifold.

I. Entire Data Collection
   a. System File.
   1. System bias; Measure residual noise with all elements turned off.
   2. Reference module; Measure output of a selected module. With all other elements turned

off, measure the complex output at the minimum attenuation and minimum phase states.
   3. Elements; For each element, with all other elements turned off, measure the complex output at the minimum attenuation and minimum phase states.
   4. Reference module; repeat step "b".
   b. Element File.
   1. Reference module; Measure output of a selected module. With all other elements turned off, measure the complex output at the maximum amplitude (minimum attenuation) state for each phase shifter setting of a single element. Next, measure the complex output at the minimum phase shifter setting for each attenuator state of the element. This generates a table of size;
$$S = N (2^{Bp} + 2^{Ba})$$
where; S = Number of complex (I & Q) measurements
   N = Number of array elements
   Bp = Number of phase shifter bits
   Ba = Number of attenuator bits

   2. Elements; Repeat step "1" for all elements.
   3. Reference module; repeat step "1".

II System-Only File
   Same as Entire File, except only the "System File" data is gathered, for fast response time.

B. Calibration
1. Correct for system bias. Subtract system bias values from each measurement in the system file and the element file.
2. System calibration drift; Compare data from the two system file reference measurements. If amplitude or phase has drifted more than a predetermined amount, halt the calibration procedure because the system has not settled. Data must be recollected. Otherwise, continue.
3. Element calibration drift; Compare data from the two element file reference measurements, for the minimum attenuation and minimum phase states. If amplitude or phase has drifted more than a predetermined amount, halt the calibration procedure because the system has not settled. Data must be recollected. Otherwise, continue.
4. Element data correction; The system data file is used to adjust the element data by shifting the entire element data file the amount indicated by the system data file, for each element. The data in this adjusted element file yields the look-up table (LUT) used for calibrated beam steering.
5. Amplitude distribution. Amplitudes in the adjusted element file are limited as follows.

Because of the nonuniformity of our modules, a uniform aperture distribution is not possible. Therefore the following procedure was developed. The goal is to make the aperture weighting symmetrical about the center of the aperture. This is done by examining maximum amplitude outputs for pairs of elements symmetrical about the center. The stronger element is then attenuated to the amplitude of the weaker element. This process raises the beam sidelobes, but optimizes power gain for the condition of modules available to us.

6. Broadside phase. Adjust the output phase of each element as closely as possible to zero. This is accomplished by selecting out of the LUT the phase shifter setting that most closely produces zero output phase for each element, to the least significant bit accuracy of the LUT. These phase settings and the amplitude settings of the previous step produce a broadside beam.

Use of Calibration.

The element adjusted table of step 4 above forms the calibration LUT used for beam steering as follows. A beam steering algorithm relates output phase, Φ of each element required to steer the beam in a given azimuth and elevation direction. The LUT is then entered to find the phase that most closely equals the required phase (I&Q) value for each element, at the amplitude setting determined above in step 5. This provides the input phase required for commands to each module.

REFERENCES

1. Strategic Defense Initiative, Department of Defense, Technical Requirements Document (TRD) for ENDO LEAP, TRD-EL-001, Revision 2, Oct 1991.
2. Empirical data provided by R. Miller, of Hughes Aircraft Co. Mr. Miller is now with Malibu Research, Calabasas, CA.
3. David N. McQuiddy, et al, "Transmit/Receive Module Technology for X-Band Active Array Radar", in Proc. IEEE, Vol 79, No. 3, March 1991, pp 308-341.
4. E. A. Jaska, et al, "Phased-Array Beampointing Error and Calibration", in Georgia Tech Research Institute Technical Journal, Vol 1, 1991, pp 21-45.
5. T. J. Lyon, "Electrical Evaluation of Operational Radomes", in Radome Engineering Handbook, J. D. Walton, Jr. ed. New York, Marcel Dekker, Inc., 1970, pp 407 to 410.
6. Josh T. Nessmith and Willard T. Patton, "Tracking Antennas", Chapter 34 in Antenna Engineering Handbook, Johnson & Jasik, ed. second ed. New York, McGraw Hill, 1984, pp 34-20 to 34-21.
7. Josh T. Nessmith and Willard T. Patton, "Tracking Antennas", Chapter 34 in Antenna Engineering Handbook, Johnson & Jasik, ed. second ed. New York, McGraw Hill, 1984, pp 34-6 to 34-7.
8. Burrell R. Hatcher, "Granularity of Beam Positions in Digital Phased Arrays", in Proc. IEEE, Vol 56, No 11, Nov 1968, pp 1795-1800.
9. J. Frank, "Beam Steering Increments for a Phased Array", in IEEE Trans. on Antennas and Propagation, Nov 1967, pp 820-821.
10. Theodore C. Cheston and Joe Frank, "Phased Array Radar Antennas,", Chapter 7, in Radar Handbook, Second Edition, ed. Merrill I. Skolnik, New York, McGraw-Hill, 1990.
11. White and Overfelt, Naval Air Warfare Center Weapons Division, China Lake, in an undocumented investigation.
12. John Feeman and Glenn Van Blaricum. "Monopulse Radome Error Compensation in the Presence of Aperture Blockage," (Final Report, Phase 1), Toyon Research Corp., Goleta, CA, April 1992.
13. Naval Weapons Center. "The Interaction of Cross-Polarized Radiation With a Radome," by John D. Hall and David J. White. China Lake, CA, NWC, August 1991. 83 pp. (NWC TM 6835, publication UNCLASSIFIED.)
14. United International Engineering, Inc., "Real Time Error Compensation," Albuquerque, NM, 23 Feb 1990.
15. Informal communication with Dr. Jim Wright, Colsa Company, Huntsville, AL, 18 Sept 92.
16. D. J. Yost, L. B. Weckesser, and R. C. Mallalieu, "Technology Survey of Radomes for Anti-Air Homing Missiles," Johns Hopkins University Applied Physics Laboratory, Laurel, MD, March 1980, Report Number FS-80-022, publication UNCLASSIFIED.
17. Naval Weapons Center. "NWC Active Array Demonstration Unit Control System," by Albert P. Burgstahler. China Lake, CA, NWC, September 1988, 127 pp. (NWC TP 6949, publication UNCLASSIFIED).
18. Albert P. Burgstahler, "NWC Active Array Demonstration Unit Control System," Proc. 1989 IEEE National Radar Conference, March 1989, pp 113-118.